HHS Public Access

Author manuscript

J Biomed Mater Res B Appl Biomater. Author manuscript; available in PMC 2018 July 01.

Published in final edited form as:

J Biomed Mater Res B Appl Biomater. 2017 July ; 105(5): 977–988. doi:10.1002/jbm.b.33632.

Synthesis and characterization of *in situ* forming anionic hydrogel as vitreous substitutes

Jue Liang[1], **Jessica J. Struckhoff**[1], **Hongwei Du**[1], **Paul D. Hamilton**[1], and **Nathan Ravi**[1,2,3]

[1]Department of Ophthalmology and Visual Sciences, WA University School of Medicine, Saint Louis, Missouri

[2]Department of Energy, Environmental and Chemical Engineering, WA University in St. Louis, Saint Louis, Missouri

[3]Department of Research, Veterans Affairs Medical Center, Saint Louis, Missouri

Abstract

The natural vitreous is a biological hydrogel consisting primarily of a collagen and anionic hyaluronate. It is surgically removed in many ocular diseases and replaced with fluids, gases, or silicone oils. We have been interested in developing synthetic hydrogels as vitreous substitutes. In this study, we combined the stiffness and hydrophobicity of polymethacrylamide (PMAM) and the anionic nature of poly-methacrylate (PMAA) to make copolymers that would mimic the natural vitreous. We used *bis*-methacryloyl cystamine (BMAC) to introduce thiol groups for reversible crosslink. The M_n of copolymers ranged from ~100 k to ~200 k Da (polydis-peristy index of 1.47–2.63) and their composition as determined by titration, ^{1}H NMR and disulfide test were close to the feed ratio. The reactivities of monomers were as follows: MAM > MAA ~ BMAC. Copolymers with higher MAA contents gelled faster, swelled more, and had higher storage modulus (1.5 to 100 Pa) comparable to that of the natural vitreous. We evaluated the biocompatibility of copolymers by electric cell-substrate impedance sensing (ECIS) using human retinal pigment epithelial cells, primary porcine retinal pigmented epithelial cells, human microvascular endothelial cells adult dermis, and a fibroblast line 3T3. The biocompatibility decreases as the content of BMAC increases.

Keywords

reversible crosslink; vitreous substitute; in situ forming hydrogel; ECIS

INTRODUCTION

The vitreous humor, which occupies two thirds of the volume of the eye, is a hydrogel predominantly composed of water (98–99%) and contains a small amount of solids consisting of a collagen network (rigid, helical and fibrillar) interspersed with hyaluronic acid (flexible, negatively charged, and randomly coiled). This composition and structure is hypothesized to give rise to an osmotic (swelling) pressure to hold the retina in place and

Correspondence to: N. Ravi; ravi@vision.wustl.edu.

circulates metabolites throughout the eye.[1] Vitreous-associated causes of vision loss include retinal complications and detachment associated with diabetes, macular holes, vitreous hemorrhage, hypertension, arteriosclerosis, choroidal melanoma, retinal tears, epiretinal membrane formation,[2] and ocular injuries. Treatment often involves removal and replacement of the vitreous. Currently, expanding gases, silicone oil, or silicone oils mixed with semi-fluorinated alkanes are used to replace the vitreous and reattach the retina in case of detachment. However, the disadvantages of these vitreous substitute include dispersion of gas, different density and refractive index than the natural vitreous, requirement for face-down positioning, poor contact with aqueous fluids, and lead to a risk of developing cataracts, glaucoma, band keratopathy, and corneal decompensation.[3] Natural and synthetic polymers to replace the human vitreous have not been successful enough to achieve widespread use.[1,4,5] Many attempts to develop hydrogels as vitreous substitutes have failed because they were pre-formed outside the eye, but shear-degraded during injection through a small-gauge needle, and failed to produce osmotic pressures to reattach the retina.

Our approach is to understand the design of the natural vitreous and reverse-engineer the critical aspects of it. The ideal vitreous substitute must (1) be injectable into a vitreous cavity as a solution, and then form a permanent hydrogel *in situ*; (2) match the natural vitreous' optical, physical, and viscoelastic properties to eliminate vision impairment; (3) be nontoxic and eliminate the need for further surgery for removal of the substitute; (4) additionally, the gels could serve as depots for intravitreal drug delivery.[6,7]

Polymer solutions, which can form a gel when placed in a body cavity or tissue with latent space, have potential uses as vitreous substitutes.[8–10] In many biomedical applications, including injectable tissue engineering,[11,12] minimally invasive drug delivery,[13] wound dressing,[14,15] materials that can form *in situ* hydrogels have considerable advantages.[16,17] In this technique, a premixed solution containing cross-linkable polymers, drugs, cells and/or other ingredient, is injected to fill native or potential cavities, and forms a matrix in *vivo* conforming to different shapes, which may be difficult to prefabricate. There are a variety of techniques used for implementing these *in situ* forming gels. In this work, we have introduced thiol groups into the side chains of our water-soluble copolymers. Thiol groups are easily transformed into disulfide bridges by air oxidation; these thiol containing polymers are cross-linkable under physiological conditions, and thus form a gel *in situ*.[18,19] While considering hydrogels for ophthalmic applications and vitreous substitute in particular, we have made our choices of materials taking into account their optical and mechanical properties, biocompatibility and stability, and resistance to UV and enzymatic degradation.[20,21] Biological systems are complex and therefore difficult to mimic with a single material. Thus, copolymers containing multiple types of monomers add to the flexibility of the polymer system. In this article, we have synthesized random copolymers obtained from copolymerization of methacrylamide (MAM), methyacrylic acid (MAA), and *N',N'-bis*(methylacryloyl-cystamine) (BMAC). The introduction of MAA to the copolymer system increases its anionic charge density and swell ability, and enables us to engineer materials with the mechanical properties in the range of the natural vitreous while maintaining a low copolymer concentration. The BMAC introduces the reversible cross-linkers which allow the formation of hydrogels by air-oxidation of the thiol groups. We have assessed the mechanical properties and flow behaviors of the hydrogels by rheology

measurements. We have tested the biocompatibility of the hydrogels with the thiazolyl blue tetrazolium bromide (MTT) assay and electric cell-substrate impedance sensing (ECIS). Cells viability was tested using four cells, established human retinal pigment epithelial cells (ARPE-19), primary porcine retinal pigmented epithelial cells (ppRPE), human microvascular endothelial cells, adult dermis (HMVECad), and a fibroblast line (3T3/NIH).

EXPERIMENTAL

Material

Reagents were purchased from Sigma-Aldrich unless otherwise stated. Glycine and ethylenediaminetetraacetic acid disodium salt (EDTA) were purchased from Fisher. ARPE-19 and NIH/3T3 cell lines were purchased from American Type Culture Collection. The HMVECad cell line was purchased from Life Technologies. MEM nonessential amino acids 100× solution (25–025-Cl), sodium pyruvate 100 m*M* solution (25–000-Cl), and L-glutamine 200 m*M* (25–005-Cl) were purchased from Corning.

Synthesis of poly(MAM-*co*-MAA-*co*-BMAC) copolymer

A typical procedure for copolymerization of MAM, MAA and BMAC is provided. MAA was distilled at 45°C under reduced pressure to remove the inhibitor and any impurities. MAM, MAA, and BMAC were dissolved in DMF at 20 wt %. The solution was purged with nitrogen for 20 min to remove the dissolved oxygen. A stock AIBN/DMF solution was syringed into the vial and the mixture was purged with nitrogen for another 20 min. The reaction was incubated at 60°C for 18 h. The obtained solid was suspended in DI water and the suspension was centrifuged at 2500 rpm for 10 min. The supernatant was decanted. This procedure was repeated three times to remove the DMF and was resuspended in DI water. The pH was adjusted to ~7.75 yielding a viscous mixture. Ten-molar excess of DTT was added to reduce the disulfide bonds. The mixture was stirred for 18 h and the suspension became clear and less viscous. Then the pH was adjusted to ~3. A white solid was precipitated and separated via centrifuge (4000 rpm, 6 min). The product was washed four times with a nitrogen-purged 1 m*M* HCl aqueous solution followed by washing with a 1 m*M* HCl/ethanol solution. The copolymer was washed with a nitrogen-purged 1 m*M* HCl aqueous solution again and lyophilized, yielding a white solid.

Characterizations of poly(MAM-*co*-MAA-*co*-BMAC) copolymer

The copolymers were titrated with a 0.1*N* NaOH aqueous solution using a pH meter to measure the contents of MAA. The amount of BMAC incorporated into the copolymers was measured by ^{1}H NMR spectra and a disulfide test as described previously.[22] Gel permeation chromatography (GPC) was also performed on the reduced copolymers.

Test of gelation rate, swelling capacity, rheology, and optical transparency

Copolymer solutions were prepared at desired concentrations for hydrogel formation and 3 mL of the solution was pipetted into weighed 35 mm dishes. The initial weights of the copolymers were recorded. Copolymers were allowed to be oxidized at 37°C in humidified containers. At periodic intervals aliquots were taken to monitor the oxidation process by Ellman's test. Copolymers were tested for gelling by tipping the dishes at a 45° angle. When

the material resisted flowing, they were considered to have gelled. After the copolymers had formed hydrogels and oxidation was greater than 99%, DPBS (-Ca, -Mg) was added to the dishes containing hydrogels, and gels were left at 37°C for an additional 5 days to allow equilibrium swelling. Excess PBS was then poured off; hydrogels were gently blotted dry and weighed (final weight). Swelling was determined by the change in weight from the initial weight to the final weight. Air oxidized re-gelled copolymers were analyzed for storage or elastic modulus determination using a Vilastic-3 (Austin, TX) oscillatory capillary tube rheometer with a 0.149 cm diameter tube at 37°C. Optical transparency (wavelength 200–800 nm) of the hydrogel was tested using a Biomate 3 (Thermo Scientific) at a concentration of 15 mg/mL.

Biocompatibility test

Ninety-six-well 10idf ECIS arrays were prepared according to manufacturer's instruction. Arrays were pretreated with 10 m*M* sterile cysteine in water to provide a coating for the gold electrodes via the interaction of the –SH groups with the gold surface, this increases the reproducibility of cell attachment and spreading. Tissue culture media (CDF-12) comprised of DMEM/F-12, 10% FCS, 100 U/mL penicillan, 1 mg/mL streptomycin, and 27.5 μg/mL amphotericin was added to the wells for protein absorption to the gold electrode surface. A frequency of 4000 Hz was used for monitoring growth and adherence (alpha) as at this frequency the resistance for the copolymer was minimized. Resistance measurements were chosen over complex impedance because the capacitance of the polymer complicates the impedance readings. A frequency of 400 Hz was used to analyze intercellular barrier function (Rb). ARPE-19 cells grown in CDF-12 were seeded at either 7500 or 20,000 cells/well. Cells plated at low density allows one to follow the growth of the cells, while high density plating reflects the maintenance of the monolayer and the strength of cell adhesion to the tissue culture plate and measures the formation of tight junctions while cells are exposed to the copolymers. The extraction and passaging procedures for ppRPE cells were performed as previously described by Toops *et al.*[23] ppRPE cells were grown in CDF-12 supplemented with MEM nonessential amino acids, sodium pyruvate, and L-glutamine. ppRPE were used at the first passage for this study and plated at 20,000 cells/well. HMVECad cells were grown per Life Technologies protocol and were plated at 5000 cells/well. 3T3NIH cells were grown in CDF-12 and plated at 10,000 cells/well. Twenty-four hours after seeding, the media was removed. The copolymers were dissolved in media and 150 μL of the solution was applied directly to the cells and allowed to be oxidized over time. Current was applied and monitored. Each polymer was tested in four separate experiments with a total of four cell lines, and replicates at each individual concentration point was varied from four to eight times.

Biocompatibility test of long-term diffusion

Hydrogels were formed by dissolving the lyophilized polymer at a final concentration of 15 mg/mL in CDF-12 media. 1.0 mL of the material was placed in each of a 24-well plate and allowed to gel by air oxidation at 37°C for 48 to 72 h. Concurrently, ARPE-19 cell were seeded in 1 mL of identical media without hydrogel on the apical side of collagen coated microporous (0.4 μ*M*) membranes, Millicell-CM (Teflon) 12 mm inserts; 48 h after plating, the inserts with cells were placed on the formed hydrogels. Media in the inserts was changed

twice a week, and cells were allowed to grow on the membranes for 21 days. This setup allows for diffusion out of the hydrogels and for the gel and cells to be in close proximity for a prolonged period of time. It was found that on the Teflon coated inserts, the cells grew in colonies. Pictures were taken at the end of 21 days.

RESULTS AND DISCUSSION

Effect of the ionic content

Copolymerization is a promising strategy to synthesize polymeric materials with properties that are tunable between those of the respective homopolymers. In this study, we combined the desirable properties of MAM, MAA, and BMAC to make copolymers (Scheme 1) that were suitable for use as a vitreous substitute. The MAM repeating units comprise the majority of the backbone and the ionic MAA repeating units help the copolymers to form gels at a lower concentration, maintain an appropriate elastic modulus and swell ability. BMAC was incorporated into the copolymers to introduce the pendent thiol groups, which were used as sites for reversible crosslinking. By using the reversible crosslinker, the reduced copolymer could be intensively purified and injected into the vitreous cavity in a solution, and then the copolymer could be recrosslinked by air-oxidation to form a gel *in situ*. The *in situ* formed gel is superior when compared with a preformed gel since the latter have been observed to shear degraded upon injection through a small gauge needle, and thus lose its elasticity and swelling ability that are necessary to hold the retina in place.

To study the effects of the ionic content on the properties of copolymers and their hydrogels, a series of copolymer containing 0, 5, 10 15, or 20 mol % of MAA, 2 mol % of BMAC, with MAM making up the rest of the copolymers, were synthesized. The hydrodynamic radius and Mark-Houwink-Sakurada constants α of the copolymers were calculated by the Omnisec software using a multi-detection system. A larger Mark-Houwink-Sakurada constant α reveals a more rigid polymer chain. In this article, both hydrodynamic radii and Mark-Houwink-Sakurada constants α increased with increased the ionic contents in the copolymers (Table I). We speculate that the negatively charged acrylates made the copolymer more hydrophilic, and the electrostatic repulsion generated from the ionic units made the copolymers more spread-out and increased the rigidity. The low Mark-Houwink-Sakurada constant α of the copolymer with 0 mol % of MAA is probably due to its poor solubility.

The gelation rates of copolymers containing different ionic contents were also compared. As we increased the content of MAA from 0 to 20 mol %, the time that was required for the copolymer solution to form a no-flowing hydrogel decreased from 21 days to 3 days (Table I). The hydrogel was formed by conversion of the pendent thiol groups to disulfide bonds which formed intra- or inter-chain, and only the inter-chain disulfide bonds helps the formation of a hydrogel. As mentioned above, the ionic content made the polymeric chains more rigid and spread-out. This probably lead to less intra-chain disulfide bonds and more inter-chain disulfide bonds (Figure 1), and thus enhanced the rate of gelation. It is also worthy to note that the copolymer solutions gelled overnight in deionized water while the gelation process was greatly delayed in PBS. The higher ionic strength in PBS partially screened the electrostatic repulsion among the ionic units and thus increased the flexibility

of the polymeric chains. As a result, there were more intra-chain crosslinks in PBS and the gelation was delayed. However, the gelation time of the polymer containing 20 mol % of MAA at 2 wt % is still too long so certain amount of polymer would diffuse away during the gelation time period. We are planning to introduce a second component, which would be temperature-responsive, to the hydrogel to provide fast *in situ* gelation.

Once a hydrogel was formed, the electrostatic repulsion among the ionic units would help the 3-D polymer network to resist compression. This was verified by the rheological test of the hydrogels. Figure 2 shows the frequency scans of the hydrogels containing 2 wt % of copolymers with varied MAA contents at a fixed shear strain of 15%. Generally, the storage modulus G' increased with MAA molar ratios increased from 0 to 15%, which suggested more resistance to the network compression. However, we observed that this did not continue above 15 mol % of MAA. The dramatic effect of the ionic contents on the G' of hydrogels indicated that the mechanical properties could be engineered by altering the MAA molar ratio in the copolymers. Overall, the G' of the hydrogels remained constant under the shear strain with varied frequencies applied, suggesting a stable and elastic network existing in the hydrogels. The swelling capacities of the hydrogels were measured in DI water and PBS medium at pH 7.5 (Figure 3). The swelling was much lower in PBS than in DI water as expected, and it increased with the MAA molar ratios increasing from 0 to 10% due to the enhanced hydrophilicity. However, there was not much difference between the copolymers with higher MAA contents.

Characterization of poly(MAM-*co*-MAA-*co*-BMAC) copolymers

The ionic content of the copolymer helps gelation and also allows us the form a hydrogel at lower concentrations to mimic the high water content (98–99 wt %), density (1.0053–1.0089 g/cm^3) and refractive index (1.3345–1.3348) of natural vitreous.[1] Therefore, all copolymers used for the following study contained 20 mol % of MAA, in which we varied the contents of BMAC crosslinker. Copolymers containing 2 or 6 mol % of BMAC were synthesized and characterized by aqueous GPC in the presence of DTT to prevent crosslinking. The results are listed in Table II.

The properties of a copolymer are largely affected by its microstructure. It is critical to investigate if the three monomers incorporated into the copolymer are statistically close to the feed ratio. In addition, terminating the polymerization before the monomers are completely consumed is a possible way to reduce the free radical side reactions. Therefore, 6 batches of poly(MAM-co-MAA-co-BMAC) copolymers were synthesized with various polymerization times from 1 to 18 h and characterized by GPC, titration, disulfide test and ^{1}H NMR to determine the effect of the reaction time on the MWs, yields and compositions (Table III). For ease of analysis of thiol content, the copolymers containing 6 mol % BMAC rather than 2 mol % BMAC were synthesized, and we do not expect that the relative reactivities of monomers would be affected significantly by changing their relative molar percentage.

Theoretically, the M_n does not change with increasing conversion of the monomers in a conventional free radical polymerization. Practically, this is not always true due to the change of the concentrations of the monomers and the existence of side reactions. In this

study, the M_n increased by extending the reaction time from 1 to 8 h. However, the M_n increased slower than the M_w. By extending the reaction time from 8 to 18 h, the M_n and M_w did not change significantly. Monomer conversions were estimated by the yields of the polymers, which were simply calculated by the mass of the obtained polymer over the initial mass of the monomer. Since the polymer may be lost during the purification process, monomer conversions were also determined before purification by integrating the refractive index curve from GPC. The monomer conversions measured by the two methods were fairly close (Table III), and the conversions kept increasing up to 18 h of polymerization.

Since the skeletons and steric hindrance of methacrylic acid and methacrylmide are similar, the reactivity ratio of the two monomers is mainly affected by the electronegativities of the substituents. In this study, the polymerizations were carried out in an organic solvent, DMF, in which the methacrylic acid was mainly undissociated and the reactivity was simplified. ^{1}H NMR spectra of the two monomers were investigated to compare the relative eletronegativities of the substituents. The chemical shifts of the methylene group were 6.26 and 5.68 ppm in methacrylic acid, 5.77 and 5.39 ppm in methacrylamide, respectively. The higher chemical shifts of the methylene groups in methacrylic acid suggested that the acid substituent is more electron withdrawing, and thus it is more reactive than methacrylamide. This was confirmed by the analysis of the contents of methacrylic acid in the copolymers with different reaction times, which were measured by acid-base titrations. It was found that the methacrylic acid mol % in the copolymers decreased slightly with increasing reaction time (Table III), which suggested that the methacrylic acid incorporated into the copolymers slightly faster than the other monomers. The final content of methacrylic acid (17.9 mol %) was lower than the feed amount (20 mol %). A possible explanation of this could be that the polymer chains with higher contents of MAA, which were more hydrophilic, were washed out by the purification process.

The contents of BMAC were measured by ^{1}H NMR (Figure 4) and disulfide test. The contents of BMAC were calculated from the integration ratios of its side methylene groups at 3.5 and 2.8 ppm to backbone at 1.0 to 2.3 ppm. Both ^{1}H NMR and disulfide test indicated that BMAC incorporated into the copolymers evenly.

The natural vitreous is a viscoelastic hydrogel. It acts as shock absorber and dampens vibrations. The storage modulus of a natural vitreous decreases with aging resulting in liquefaction of the vitreous. Mechanical property is one of the most critical parameters for designing a vitreous substitute. Aqueous solutions of the copolymers containing 20 mol % MAA were prepared at concentrations of 0.9, 1.35, and 1.8 wt % and were allowed to oxidize to form gels. The rheological properties of the gelled copolymers were analyzed by frequency scans (Figure 5). The storage moduli of the tested gels were independent of frequency in the range of 0.1 to 30 Hz. The copolymer containing 2 mol % BMAC resulted in gels with a storage modulus range of ~1.5 to 45 Pa, and the copolymers containing 6 mol % BMAC resulted in gels with a storage modulus range of 1.5 to 100 Pa. It is noteworthy that with increasing the concentration of the two copolymers from 0.9 to 1.8 wt %, the storage moduli increased dramatically from 1.5 to 45 and 100 Pa, respectively. Additionally, the gel with 6 mol % of BMAC had a storage modulus more than twice as much as the one with 2 mol % of BMAC at concentration 1.8 wt %. Therefore, the mechanical properties of a

gel could be adjusted by varying the concentration of the polymer and the density of the crosslinker, and thus match the mechanical properties of the natural vitreous. It is promising that the published storage modulus of the porcine and bovine vitreous[24,25] were in the range of our test values.

The hydrogel was transparent (transmittance >95%) in the visible and long-wavelength ultraviolet range (300–800 nm). Transmittance of the hydrogel in the short-wavelength ultraviolet range (under 300 nm) drops drastically to zero similar to that of the natural vitreous (Figure 6).

Cytocompatibility

ECIS is a technique that can provide electrical information, which can be interpreted in terms of cellular physiology. This real-time, non-invasive technique measures the impedance across the electrodes utilizing alternating current at various frequencies. When cells are growing on the electrodes, the impedance is affected by the number, morphology and attachment of cells covering the electrodes. The current flows through two types of pathways: (1) at low frequency, the dominant current flow is in the solution channels under and between cells, it is particularly valuable in analyzing barrier function.; (2) at high frequency, the capacitance due to the insulating cell membranes becomes the most significant pathway and it is used to analyze the density and growth of cells.

We have tested four different cell lines: two retinal pigment epithelial cell lines, including ARPE-19 cells, an established cell line of human origin, and the other, ppRPE or porcine primary cells; an endothelial or HMVEC cell line, and a fibroblast or 3T3/NIH cell line. Figure 7(a) shows the resistance measurements of ARPE-19 cells plated at high (20,000 cells/well) density exposed to the copolymer containing 2 mol % of BMAC. Initially, there was some growth and cell division. As the cells reached the maximum density, we could model these measurements to compare adherence of the cells with the substrate. It is significant to note that at the time of exposure, there was an initial difference in resistance between the treated and the control cells after the application of the copolymers. This difference was also correlated to the amount of copolymers present. It could be because oxygen was depleted from the media as the copolymer was oxidized and this might cause a slowing in cell growth. The resistance indicated that the cell growth and attachment increased with time in a manner similar to the control cells up to a concentration of 10 mg/mL, with a slight decrease at 15 mg/mL. ARPE-19 cells plated at low density continued to divide and did not reach a maximum density throughout the course of the experiment [Figure 7(b)]. These cells plated at low density showed a more pronouced effect from the copolymers on the growth curve of cells than the ARPE-19 cells plated at high density. There was initially a significant decrease in resistance at 15 mg/mL with the copolymer containing 2 mol % of BMAC. However, the resistance continued to increase, indicating sustained but slowed growth of the cells over the gold electrodes. The ppRPE cells [Figure 7(c)] and HMVECad cells [Figure 7(d)] exhibited similar response to the copolymers as the ARPE-19, and showed only a small resistance decrease at 15 mg/mL. The fibroblast 3T3/NIH cells gave a significantly lower resistance measurement than the other cell types [Figure 7(e)]. ECIS analysis of the 3T3/NIH cell line showed the most inhibition of cell

growth in the presence of the copolymers. To demonstrate the interference of thiol-containing copolymer to the resistance measurement, the cysteine-pretreated gold electrodes were exposed to the solutions of copolymer and media only for comparison. The resistance patterns of the copolymer solution overlapped the resistance pattern of the media only [Figure 7(f)] which suggests that the interference of the copolymer containing 2 mol % of BMAC is insignificant at the tested concentration.

However, the high density ARPE-19 cells exposed to the copolymer containing 6 mol % of BMAC only compared well to the controls at or below 10 mg/mL [Figure 8(a)]. At 12.5 mg/mL and above, the resistance values were significantly lower compared with the controls. The resistance of the low density ARPE-19 exposed to the copolymer containing 6 mol % of BMAC at 10 and 15 mg/mL stopped increasing after polymer addition [Figure 8(b)]. However, when combining this information with the pictures of the cells [Figure 8(b)], the morphology of the cells appeared fairly normal, though there was a noticeable reduction in cell number. Again, with the copolymer containing 6 mol % of BMAC, the ppRPE cells [Figure 8(c)], HMVECad cells [Figure 8(d)] and 3T3/NIH cells [Figure 8(e)] showed a significant decrease in resistance at both 10 and 15 mg/mL. They also showed increased deleterious effects with the copolymer containing 6 mol % of BMAC when compared with the copolymer containing 2 mol % of BMAC above 10 mg/mL. Again, the resistance patterns of copolymer solution containing 6 mol % of BMAC overlapped the resistance pattern of the media only [Figure 8(f)]. Therefore, the interference of the copolymer containing 6 mol % of BMAC is also insignificant at the tested concentration.

All four cell lines indicated that there was a significant difference in biocompatibility between the copolymer containing 2 and 6 mol % of BMAC, with the cells responding much more favorably to copolymer containing 2 mol % of BMAC. The increase in the thiol-containing cross-linker did not significantly affect the storage modulus of the oxidized gels at concentrations up to 13.5 mg/mL. Therefore the better biocompatibility of the copolymer containing 2 mol % of BMAC outweighs any advantage that the higher cross-link density may provide.

When observing the morphology of the ARPE-19 cells plated at high density [Figure 9(a)], we did not pick up significant differences between the control cells and the cells exposed to the copolymers. However, the resistance results [Figure 8(a)] indicated that the copolymer containing 6 mol % of BMAC was deleterious to the cell monolayer. The low density ARPE-19 cells exposed the copolymer containing 6 mol % of BMAC at 15 mg/mL had fewer cells compared with the control cells while the mophology remained unchanged [Figure 9(b)]. The density and morphology of ppRPE cell that were exposed to both copolymers at 15 mg/mL appeared similar to control cells [Figure 9(c)]. HMVECad cells showed some rounding and also some vacuoles [Figure 9(d)]. Pictures of the 3T3/NIH cells after 72 h of exposure to the copolymers [Figure 9(e)] also indicated that cell growth was inhibited, and this inhibition was significant, especially with the copolymer containing 6 mol % of BMAC.

MTT assays were performed as viability assays for the polymers and as a comparison to the ECIS results. However, it appears that the ionic polymers (containing methacrylate) have a

certain measure of adhesion with the cells, petri dishes and MTT dye, making it difficult to remove the extracellular dye completely. The results gave viability that actually registered higher than 100%. We concluded that the gel that adhered, contributed/interfered with the color formation. We have other colorimetric assays with equally problematic results. Other publications have favorably compared the results of MTT and ECIS.[26,27] ECIS produces much more data and provides unbiased information of changes in impedance/resistance for the time course of the cellular response. Responses are based on cell density and changes in cell morphology that are associated with cell death. The response can be modeled to show adhesion and barrier responses in addition to cell growth.

Test of barrier function

The RPE cells, located between the retina and the choroid, form tight junctions, which are responsible for the blood-retinal barrier between the retina and the choroid vasculature. Since the primary purpose for our copolymers is for use as a vitreous substitute, we are particularly interested in the effect on the barrier function of RPE cells. At low frequencies, the ECIS instrument detects the formation of tight junctions between the RPE cells. Using the provided software at 400 Hz, the barrier function Rb measurement was modeled for ARPE-19 cells (Figure 10). The results closely followed the resistance data. It is highly relevant that with the copolymer containing 2 mol % of BMAC the tight junctions appeared to form well up through a concentration of 12.5 mg/mL. While at 15 mg/mL the ARPE-19 cells continue to have a sustained but diminished increase in resistance over 4 days of exposure. However, the values continued to increase with time. This copolymer starts forming a gel network at approximately 10 mg/mL. It appears that the optimum concentration to use as a vitreous substitute will be from 10 to 12.5 mg/mL. Below this concentration, the copolymer will not gel and above this concentration, it begins to show toxicity.

With the copolymer containing 6 mol % of BMAC, resistance modeled for tight junction values showed a significant decrease in resistance at and above 12.5 mg/mL, indicating that at these concentrations, the tight junction formation was disrupted by either toxicity or the gel physically separating the cells.

Biocompatibility test of long-term diffusion

In the purification process of the polymer material, after reduction with DTT, the reduced solution was dialyzed exhaustively using a MWCO = 12–14 kDa membrane, greatly reducing any probability of low molecular weight contaminants or diffusible material. However, to check for any leaching of materials that could influence biocompatibility, the cells were grown on a semipermeable membrane with 0.4μM pore size where the membrane is in direct contact with the formed polymer gel at a concentration of 15 mg/mL. This is the highest concentration we intend on using in our vitreous applications. In this experimental condition, the cells can be grown and remain viable for a prolonged period of time in close proximity to the polymer gel. Cell growth was observed >21 days. No toxic effects were observed at any time, and cell growth/colony formation between the control cells and cells in the presence of polymer was equal to or better than control cells with no polymer present (Figure 11).

CONCLUSION

We have reported the synthesis of a three-component poly(-MAM-*co*-MAA-*co*-BMAC) copolymer that can be injected in to the vitreous cavity as a solution and then form an anionic hydrogel *in situ* as a bio-mimic vitreous substitute. We determined that the thiol-containing BMAC incorporated into the copolymer evenly while MAA reacted slightly faster than the others. We were able to tailor the composition and molecular weight of the copolymer by varying the formulation of polymerization. We also determined that the ionic MAA component has great impact on the polymer chain flexibility and the formation rate, mechanical property, and swelling capability of the hydrogel. The storage modulus of the hydrogel was altered to match the natural vitreous by changing concentration of the copolymer and thiol content. We determined that the copolymer containing 2 mol % of BMAC is more biocompatible than 6 mol % of BMAC in all four cell lines. ARPE-19 cells tolerated the copolymer containing 2 mol % of BMAC up to a concentration of 12.5 mg/mL. Therefore, our preliminary results suggest that the *in situ* forming anionic hydrogel is a promising material to be used as a vitreous substitute. Further assessments of this material, such as *in vivo* test, are underway.

Acknowledgments

Contract grant sponsor: NIH Core Grant; contract grant number: P30 EY02687

Contract grant sponsor: NIH Grant; contract grant number: EY021 620

Contract grant sponsor: Research to Prevent Blindness, Inc.

Contract grant sponsor: Department of Veterans Affairs Rehab Merit Review; contract grant number: RX000657-01

References

1. Swindle KE, Ravi N. Recent advances in polymeric vitreous substitutes. Expert Rev Ophthalmol. 2007; 2:255–265.
2. Los LI, van der Worp RJ, van Luyn MJA, Hooymans JMM. Age-related liquefaction of the human vitreous body: LM and TEM evaluation of the role of proteoglycans and collagen. Investigat Ophthalmol Vis Sci. 2003; 44:2828–2833.
3. Federman JL, Schubert HD. Complications associated with the use of silicone oil in 150 eyes after retina-vitreous surgery. Ophthalmology. 1988; 95:870–876. [PubMed: 3174036]
4. Nakagawa M, Tanaka M, Miyata T. Evaluation of collagen gel and hyaluronic acid as vitreous substitutes. Ophthal Res. 1997; 29:409–420.
5. Hong Y, Chirila TV, Vijayasekaran S, Shen WY, Lou X, Dalton PD. Biodegradation in vitro and retention in the rabbit crosslinked poly(1-vinyl-2-pyrrolidinone) hydrogel as a vitreous substitute. J Biomed Mater Res. 1998; 39:650–659. [PubMed: 9492228]
6. Laude A, Tan LE, Wilson CG, Lascaratos G, Elashry M, Aslam T, Patton N, Dhillon B. Intravitreal therapy for neovascular age-related macular degeneration and inter-individual variations in vitreous pharmacokinetics. Progr Retinal Eye Res. 2010; 29:466–475.
7. Kang Derwent JJ, Mieler WF. Thermoresponsive hydrogels as a new ocular drug delivery platform to the posterior segment of the eye. Trans Am Ophthalmol Soc. 2008; 106:206–214. [PubMed: 19277236]
8. Chirila TV, Tahija S, Hong Y, Vijayasekaran S, Constable IJ. Synthetic polymers as materials for artificial vitreous body: review and recent advances. J Biomater Appl. 1994; 9:121–137. [PubMed: 7782996]

9. Hogen-Esch TE, Shah KR, Fitzgerald CR. Development of injectable poly(glyceryl methacrylate) hydrogels for vitreous prosthesis. J Biomed Mater Res. 1976; 10:975–976. [PubMed: 993232]
10. Suri S, Banerjee R. In vitro evaluation of in situ gels as short term vitreous substitutes. J Biomed Mater Res Part A. 2006; 79:650–664.
11. Cao LP, Cao B, Lu CJ, Wang GW, Yu L, Ding JD. An injectable hydrogel formed by in situ cross-linking of glycol chitosan and multi-benzaldehyde functionalized PEG analogues for cartilage tissue engineering. J Mater Chem B. 2015; 3:1268–1280.
12. Wan WB, Li QT, Gao HY, Ge LP, Liu YQ, Zhong W, Ouyang J, Xing M. BMSCs laden injectable amino-diethoxypropane modified alginate-chitosan hydrogel for hyaline cartilage reconstruction. J Mater Chem B. 2015; 3:1990–2005.
13. Chen C, Wang L, Deng LD, Hu RJ, Dong AJ. Performance optimization of injectable chitosan hydrogel by combining physical and chemical triple crosslinking structure. J Biomed Mater Res Part A. 2013; 101:684–693.
14. Lee Y, Bae JW, Lee JW, Suh W, Park KD. Enzyme-catalyzed in situ forming gelatin hydrogels as bioactive wound dressings: Effects of fibroblast delivery on wound healing efficacy. J Mater Chem B. 2014; 2:7712–7718.
15. Sakai S, Tsumura M, Inoue M, Koga Y, Fukano K, Taya M. Polyvinyl alcohol-based hydrogel dressing gellable on-wound via a co-enzymatic reaction triggered by glucose in the wound exudate. J Mater Chem B. 2013; 1:5067–5075.
16. Ko DY, Shinde UP, Yeon B, Jeong B. Recent progress of in situ formed gels for biomedical applications. Progr Polym Sci. 2013; 38:672–701.
17. Yu L, Ding JD. Injectable hydrogels as unique biomedical materials. Chem Soc Rev. 2008; 37:1473–1481. [PubMed: 18648673]
18. Chong SF, Chandrawati R, Stadler B, Park J, Cho J, Wang YJ, Jia ZF, Bulmus V, Davis TP, Zelikin AN, Caruso F. Stabilization of polymer-hydrogel capsules via thiol-disulfide exchange. Small. 2009; 5:2601–2610. [PubMed: 19771568]
19. Yang F, Wang J, Cao LY, Chen R, Tang LJ, Liu CS. Injectable and redox-responsive hydrogel with adaptive degradation rate for bone regeneration. J Mater Chem B. 2014; 2:295–304.
20. Aliyar HA, Hamilton PD, Ravi N. Refilling of ocular lens capsule with copolymeric hydrogel containing reversible disulfide. Biomacromolecules. 2005; 6:204–211. [PubMed: 15638522]
21. Swindle-Reilly KE, Shah M, Hamilton PD, Eskin TA, Kaushal S, Ravi N. Rabbit study of an in situ forming hydrogel vitreous substitute. Investig Ophthalmol Vis Sci. 2009; 50:4840–4846. [PubMed: 19324846]
22. Thannhauser TW, Konishi Y, Scheraga HA. Analysis for disulfide bonds in peptides and proteins. Methods Enzymol. 1987; 143:115–119. [PubMed: 3657523]
23. Toops KA, Tan LX, Lakkaraju A. A detailed three-step protocol for live imaging of intracellular traffic in polarized primary porcine RPE monolayers. Exp Eye Res. 2014; 124:74–85. [PubMed: 24861273]
24. Nickerson CS, Park J, Kornfield JA, Karageozian H. Rheological properties of the vitreous and the role of hyaluronic acid. J Biomech. 2008; 41:1840–1846. [PubMed: 18534603]
25. Nickerson CS, Karageozian HL, Park J, Kornfield JA. Internal tension: A novel hypothesis concerning the mechanical properties of the vitreous humor. Macromol Symp. 2005; 227:183–189.
26. Kling B, Bucherl D, Palatzky P, Matysik FM, Decker M, Wegener J, Heilmann J. Flavonoids, flavonoid metabolites, and phenolic acids inhibit oxidative stress in the neuronal cell line HT-22 monitored by ECIS and MTT assay: A comparative study. J Nat Prod. 2014; 77:446–454. [PubMed: 24245939]
27. Yun YH, Dong ZY, Tan ZQ, Schulz MJ. Development of an electrode cell impedance method to measure osteoblast cell activity in magnesium-conditioned media. Anal Bioanal Chem. 2010; 396:3009–3015. [PubMed: 20213174]

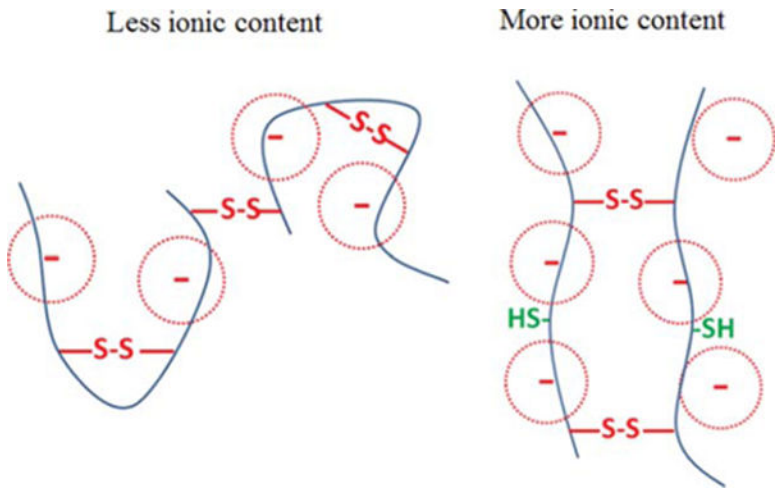

FIGURE 1.

A schematic illustration of increased chain rigidity and inter-chain crosslink with more ionic contents.

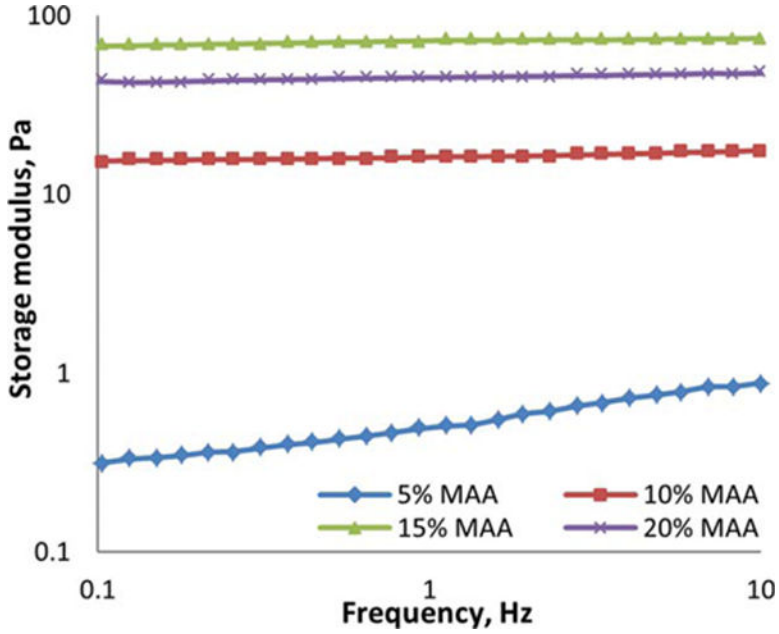

FIGURE 2.

A double-logarithmic plot of the frequency dependence of storage modulus (G') of the hydrogels obtained from 2 wt % copolymers with varied MAA molar ratios at room temperature.

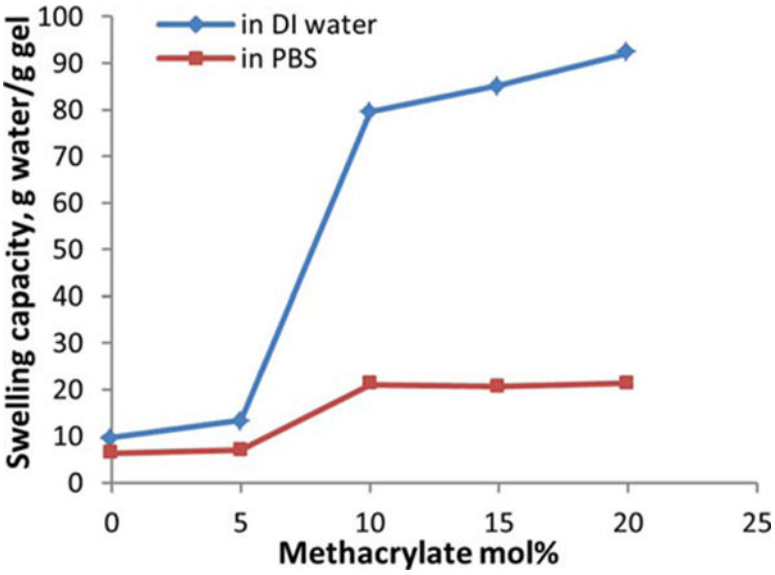

FIGURE 3.

The influence of the molar ratio of MAA in the copolymers on the swelling capacity of the hydrogels in DI water and PBS at room temperature.

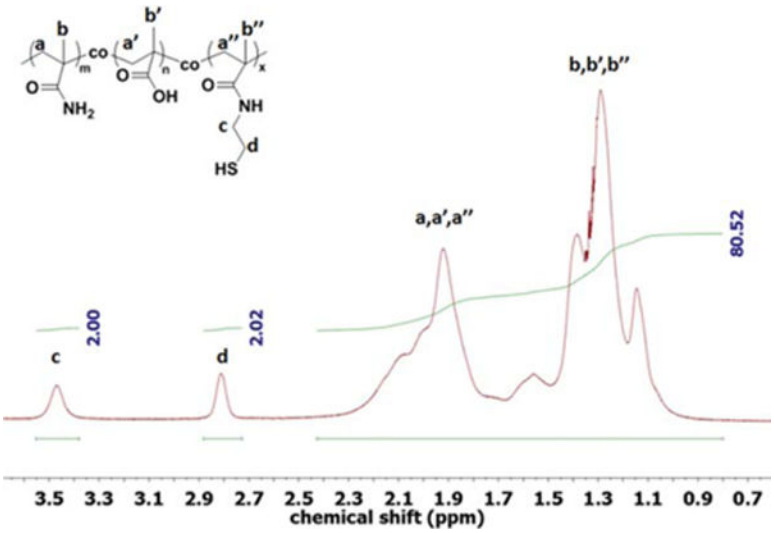

FIGURE 4.

A ^{1}H NMR spectrum of poly(MAM-*co*-MAA-*co*-BMAC) copolymer in D_2O.

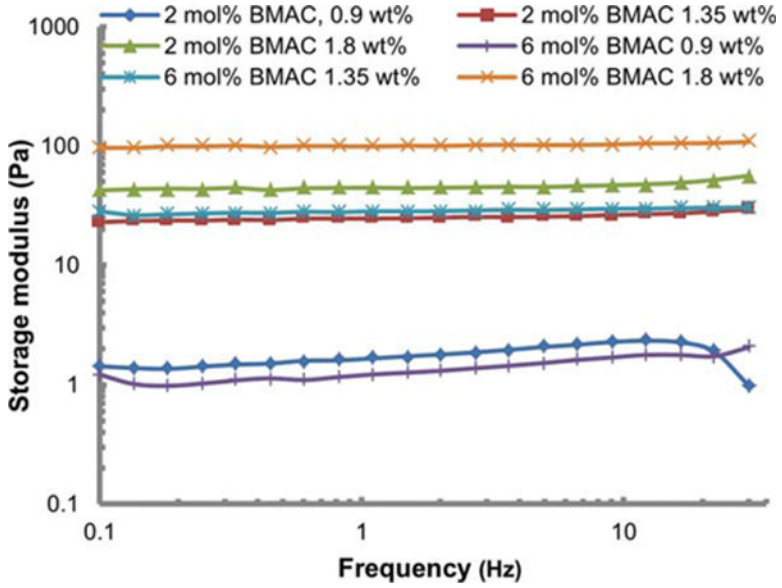

FIGURE 5.

Storage modulus of gels formed by copolymers containing 2 or 6 mol % of BMAC at 0.9, 1.35, and 1.8 wt %.

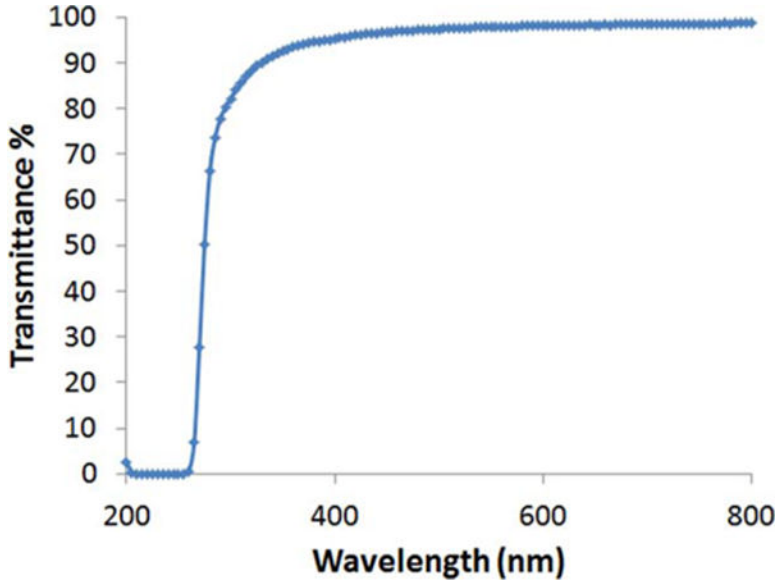

FIGURE 6.
Optical transmittance of the hydrogel (15 mg/mL) at wavelength from 200 nm to 800 nm.

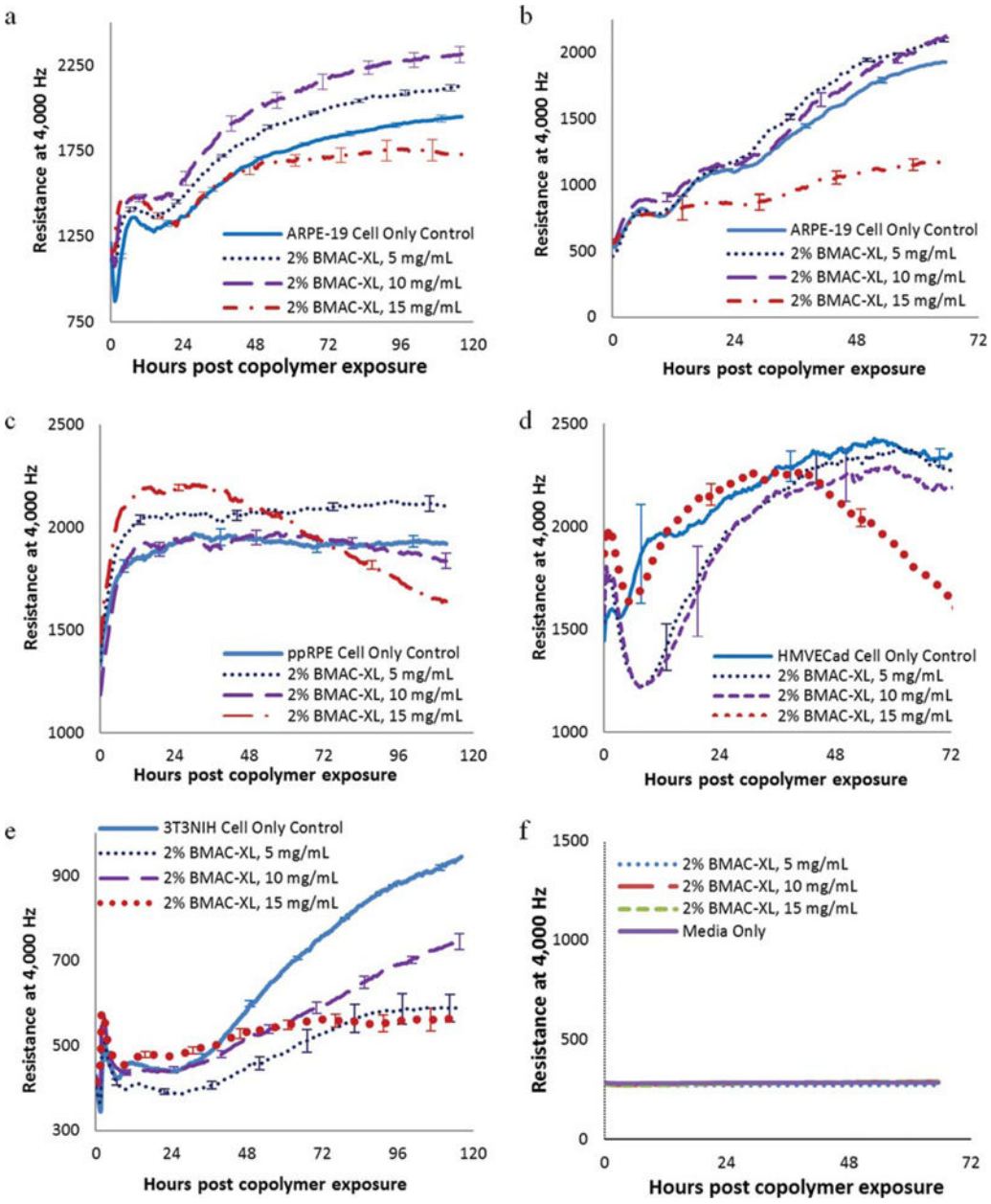

FIGURE 7.

Comparison of resistance measurements of (a) ARPE-19 cells plated at high density (20,000 cells/well), (b) ARPE-19 cells plated at low density (7500 cells/well), (c) ppRPE cells (20,000 cells/well), (d) HMVEC cells (5000 cells/well), (e) 3T3NIH cells (10,000 cells/well) exposed to copolymer containing 2 mol % of BMAC. Each data point represents the average of three or four wells, and error bars represent the standard error as established by the standard deviation divided by the square root of the well number.

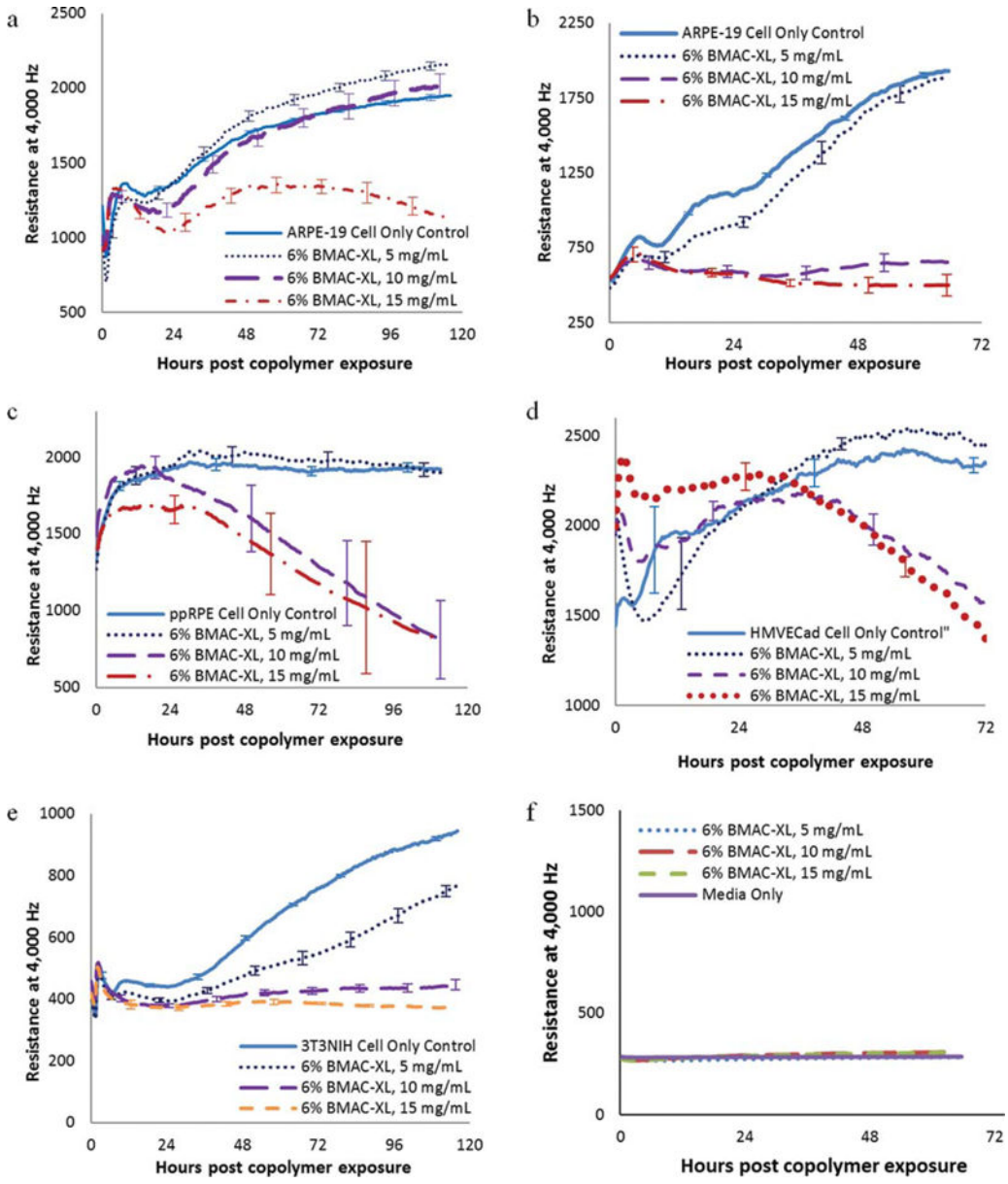

FIGURE 8.

Comparison of resistance measurements of (a) ARPE-19 cells plated at high density (20,000 cells/well), (b) ARPE-19 cells plated at low density (7,500 cells/well), (c) ppRPE cells (20,000 cells/well), (d) HMVEC cells (5,000 cells/well), (e) 3T3NIH cells (10,000 cells/well) exposed to copolymer containing 6 mol % of BMAC. Each data point represents the average of three or four wells, and error bars represent the standard error as established by the standard deviation divided by the square root of the well number.

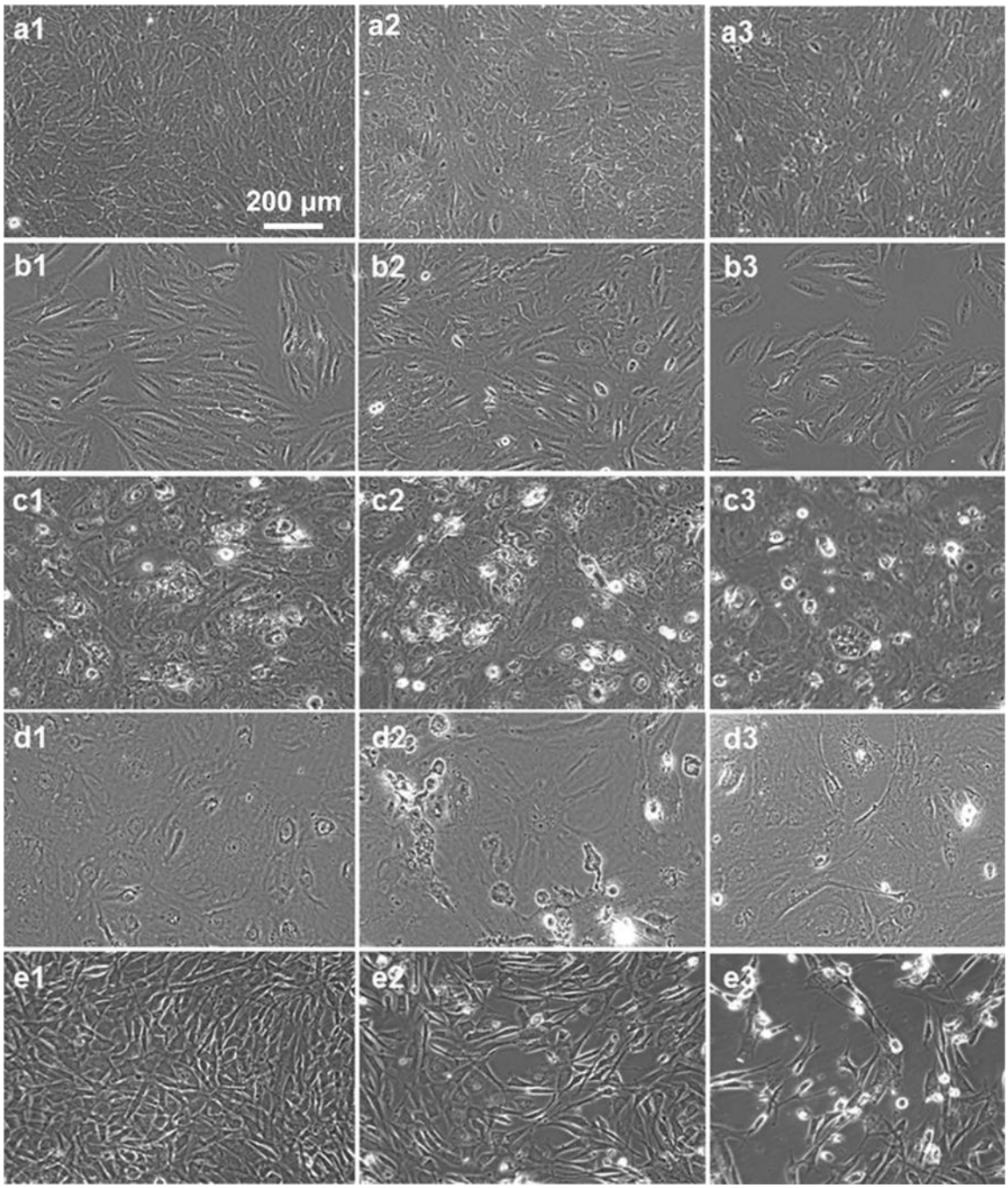

FIGURE 9.

(a1–a3) ARPE-19 cells from high density experiment (20,000 cells/well initial), (b1–b3) ARPE-19 cells from low density experiment (7500 cells/mL initial), (c1–c3) ppRPE cells (20,000 cells/mL initial), (d1–d3) HMVEC cells (5000 cells/ml initial), (e1–e3) 3T3NIH cells (10,000 cells/ well initial): (×1) control cells, (×2) cells exposed to copolymer containing 2 mol % of BMAC at 15 mg/mL, (×3) cells exposed to copolymer containing 6 mol % of BMAC at 15 mg/mL, after 72 h of exposure.

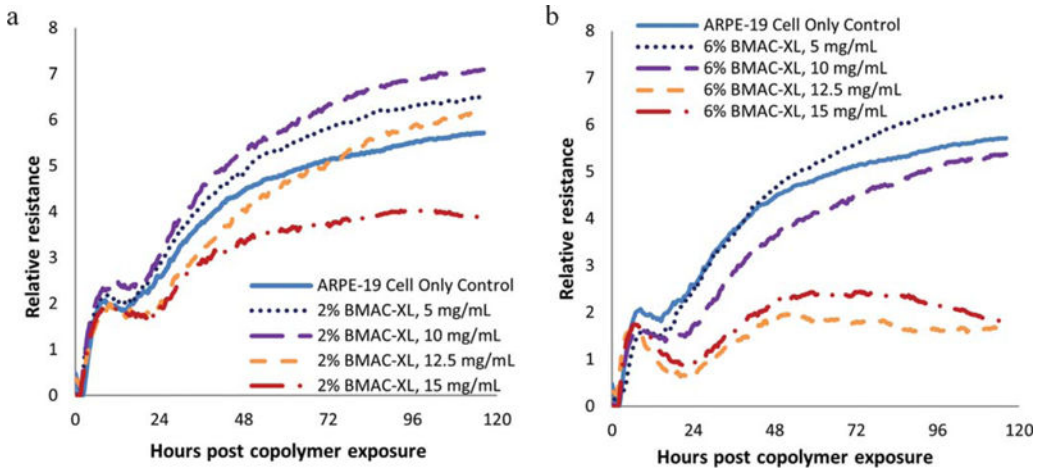

FIGURE 10.

Comparison of modeled tight junction (Rb) measurements of ARPE-19 cells plated at high density (20,000 cells/well) and exposed to copolymers containing 2 (a) and 6 (b) mol % of BMAC.

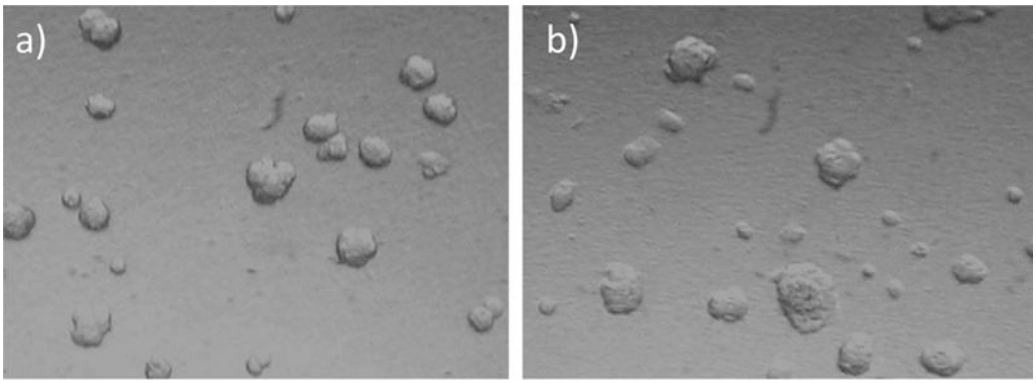

FIGURE 11.

ARPE-19 cells were grown on the apical side of microporous (0.4μm) membranes with (a) control media; (b) hydrogel (15 mg/mL) on the other side. Pictures were taken at 3 weeks.

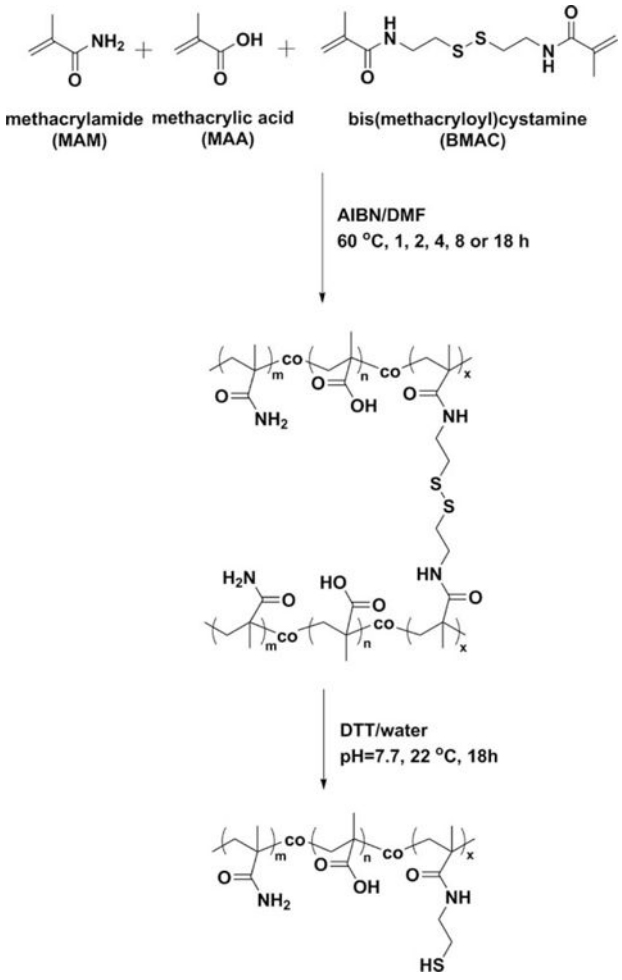

SCHEME 1.
Copolymerization of MAM, MAA and BMAC.

TABLE I

The Influence of the Molar Ratio of MAA in the Copolymers on the Hydrodynamic Radius, Mark-Houwink-Sakurada Constant A and Gelation Time

MA (mol %)	Hydrodynamic Radius (nm)	Mark-Houwink-Sakurada Constant: A	Gelation Time (d)
0	8.8	0.023	21
5	11.6	0.717	14
10	16.0	0.921	11
15	23.3	0.902	7
20	23.7	1.230	3

TABLE II

Molecular Weights of Poly(MAM-*co*-MAA-*co*-BMAC) Copolymers Measured by GPC

Entry	Mol % of BMAC	Initiator:Monomer mole:mole	M_n	M_w	PDI	DP	Yield%
1	2	1:385	98.7 k	260 k	2.63	1142	81
2	2	1:770	237 k	348 k	1.47	2741	84
3	6	1:373	224 k	475 k	2.12	2520	79

J Biomed Mater Res B Appl Biomater. Author manuscript; available in PMC 2018 July 01.

TABLE III

Characterizations of Poly(MAM-*co*-MAA-*co*-BMAC) (Molar Ratio = 74:20:6) Copolymers with Different Polymerization Times

				Monomer Conversion			BMAC mol %	
Reaction Time/h	M_n	M_w	PDI	By GPC	By Yield	MAA mol %	By ^{1}H NMR	By S-S Test
1	87 k	138 k	1.70	26	19	20.3	6.3	7.1
2	150 k	210 k	1.40	29	23	19.4	6.2	6.6
4	166 k	347 k	2.10	53	60	18.5	6.2	6.7
8	213 k	495 k	2.33	65	70	18.5	6.1	7.7
18	224 k	475 k	2.12	86	79	17.9	6.2	7.7

J Biomed Mater Res B Appl Biomater. Author manuscript; available in PMC 2018 July 01.